ISSN (Print) 1226-1750
ISSN (Online) 2233-6656
Journal of Magnetics 27(1), 18-27 (2022) https://doi.org/10.4283/JMAG.2022.27.1.018

Investigation of Torque Ripple in an Induction Motor with Respect to Slot Number Combinations

Yongha Choo[1], Changhwan Kim[1], Gyeonghwan Yun[1], and Cheewoo Lee[1]*

[1]*Department of Electrical and Computer Engineering, Pusan National University, Busan 46241, Republic of Korea*

(Received 17 December 2021, Received in final form 29 March 2022, Accepted 29 March 2022)

In this study, the harmonic orders of varying magnetic flux density with respect to slot combinations are scrutinized through a spatial and temporal fast Fourier transform. A three-phase four-pole induction motor is selected, and, as its base model, 36 and 28 slots are set up in the stator and rotor, respectively. Eleven models with different numbers of rotor slots were designed to study torque ripples with respect to slot combinations. The correlation between torque ripple and slot harmonics in a stator and rotor is described thoroughly by comparing the tangential and radial magnetic flux densities in the air gap, tangential force density, and harmonic orders in torque. Some models having deteriorated torque ripples have one or more slot harmonic orders in common in the stator and rotor. The other models exhibit the same commonalities, but a small torque ripple occurs because of the high harmonic orders. Models with 24 stator slots are investigated through the same procedure to generalize the relationship between torque ripple and slot harmonics in 36 stator slots.

Keywords : Induction motor, torque ripple, flux density, slot combination

1. Introduction

Because induction motors have been used in various industrial fields for over 100 years, many researchers have become increasingly aware of performance improvements. To improve efficiency, the air gap in induction motors is relatively narrower in comparison with that of other types of motors, but harmonic waves increase for this reason. Be-cause the harmonic components are directly related to not only torque ripple and might be connected to vibration and noise, the reduction of torque ripple is essential for performance improvement in induction motors. Several studies have been conducted on torque ripple; these include the study of the effect of harmonics generated by slot combinations on magnetic flux density in the air gap [1], research on the effect of distorted magnetic flux density on torque and its ripple [2, 3], and the analysis of varying performances with respect to slot combinations [4-8]. Most studies on slot combinations analyze torque ripple by simply checking the magnitude of magnetic flux density in the air gap and the harmonic order, but the direct correlation between them has not been clearly investigated in the literature. In this study, varying magnetic flux density in the air gap and the harmonic order with respect to slot combinations were identified, and the effect of harmonic order on torque ripple was analyzed to investigate the relationship between them.

*Corresponding author: Tel: +82-51-510-7377
Fax: +82-51-513-0212, e-mail: cwlee1014@pusan.ac.kr

2. Slot Harmonic Order

The harmonic orders of the magnetomotive force are determined by the number of slots in a motor, and the magnetic flux density in the air gap is distorted in proportion to the magnitude of the harmonics. A slot combination between a stator and a rotor directly affects the magnitude and order of slot harmonics. In particular, the order of the slot harmonics in the stator is determined as

$$h_s = 2m_1q_1k\pm1 = 2m_1\frac{N_s}{m_1(2p_1)}k\pm1 = \frac{N_s}{p_1}k\pm1\,. \qquad (1)$$

In equation (1), the order of harmonics is dependent on the number of stator slots (N_s), phases (m), and pole pairs (p) in the stator [9]. Here, q_1 and k are the number of stator slots per pole in one phase and a positive integer, respectively. The order of the slot harmonics in the rotor is determined as

Table 1. Calculation results from equations (1) and (2).

		f_s			f_r		
Stator	Rotor	$k=1$	$k=2$	$k=3$	$k=1$	$k=2$	$k=3$
36	28	17, 19	35, 37	53, 55	13, 15	27, 29	41, 43

$$h_r = (2m_2q_2k(1-slip)\pm 1) = \left(k(1-slip)\frac{N_r}{p_1}\pm 1\right), \quad (2)$$

where q_2, N_r, and m_2 are the number of rotor slots per pole in one phase, the number of rotor slots, and number of phases, respectively.

In the case of zero slip in an induction motor having a 36-slot stator and a 28-slot rotor, the order of slot harmonics calculated by using equations (1) and (2) are given in Table 1 by considering k up to 3. Torque performance is determined by electromagnetic characteristics in an induction motor, and hence, the electromagnetic deterioration of a certain harmonic order has an impact on torque ripple in some cases. By analyzing the variation of harmonics in terms of the slot combination, the harmonic orders that dominate the torque ripple can be identified. In this study, the relationship between the slot harmonic and torque ripple is investigated by changing the rotor slot number with a fixed 36-slot stator.

3. Design of Rotor Slots for Comparison and Analysis

In this study, a three-phase four-pole induction motor was selected, and as its base model, the stator and rotor were outfitted with 36 and 28 slots, respectively. Fig. 1 shows the cross-sectional view of the base and its specifications. The motor was estimated at the rated condition of 7.5 kW to have an efficiency of 92.6 %, which is more than the IE3 premium grade of 91.7 %. As indicated in Table 2, the number of rotor slots was varied from a

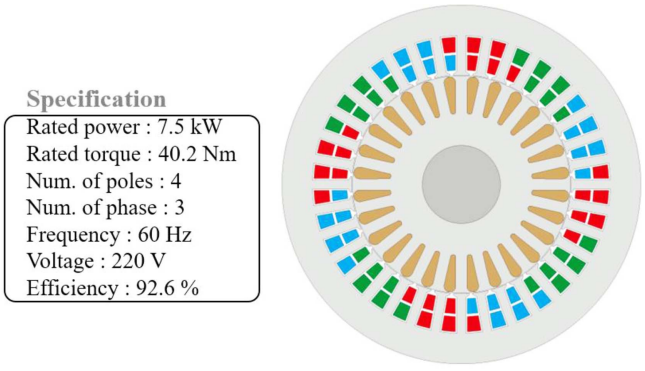

Fig. 1. (Color online) Specification and cross-sectional view for a base model.

Table 2. Combination of 36 stator slots for the comparative study.

Number of poles	Number of slots in stator	Number of slots in rotor
4	36	26, 28, 30, 32, 34, 38, 40, 42, 44, 46, 48

minimum of 26 to 48 slots in intervals of two slots for comparison, and the range of the slot number was based on a previous study [9].

The 11 models having the same magnetic flux density in a rotor tooth and yoke were designed to have identical performance to the rotor of the base model. Because the total flux in all rotor teeth is nearly equal to the total magnetic flux in the air gap, the magnetic flux density in the induction motor is given by

$$B_{gm}\tau_r L \approx B_{tr}b_{tr}Lk_{is}, \quad (3)$$

where B_{gm}, B_{tr}, τ_r, b_{tr}, and k_{is} are the magnetic flux density in the air gap, magnetic flux density in the rotor teeth, slot pitch of the rotor, width of the rotor tooth, and stacking factor, respectively. The width of a rotor tooth (b_{tr}) is determined by the slot pitch in the rotor (τ_r) because the two flux densities and the stacking factor are integers. The slot pitch of a rotor (τ_r) can be calculated using the outer diameter (D_{or}) and the number of slots for the rotor (N_r):

$$\tau_r = \frac{\pi D_{or}}{N_r}. \quad (4)$$

The height (h_{cr}) of a rotor yoke, with the maximum value of the magnetic flux density in the air gap and flux density in the yoke (B_{cr}), can be expressed as [10]

$$h_{cr} = \frac{B_{gm}\tau_p}{2B_{cr}}, \quad (5)$$

where τ_p is the pole pitch. In this study, the cross-sectional area of all rotor bars and magnetic flux density in the teeth and yokes for 11 models were designed equally with the base model by calculating with equations (3), (4), and (5) to observe variations by using different slot combinations. Fig. 2 shows the cross-sectional views of the 11 models with the same magnetic flux density in the teeth and yokes.

4. Analysis of Torque with Respect to Slot Combinations

The tangential force density (F_t) can be calculated from the tangential (B_t) and radial (B_r) flux densities as follows [11].

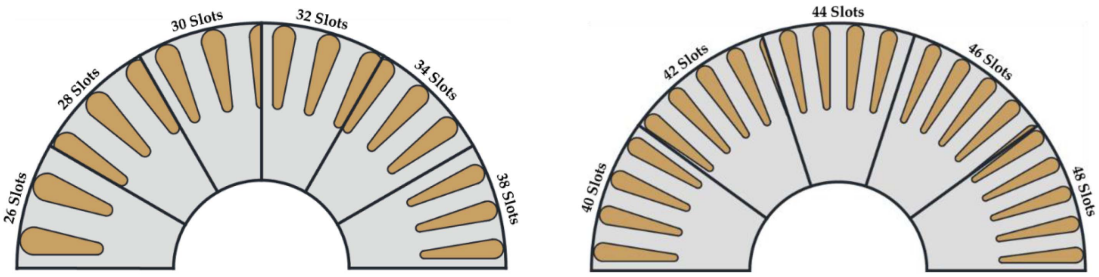

Fig. 2. (Color online) Eleven models with different numbers of rotor bars: (a) 26, 28, 30, 32, 34, and 38 slots; (b) 40, 42, 44, 46, and 48 slots.

$$F_t(t,\ \theta) = \frac{B_r(t,\ \theta)B_t(t,\ \theta)}{\mu_0} \tag{6}$$

and B_r are spatially (θ) distributed along the motor construction, and the spatial distributions of the two flux densities are temporally (t) changed by the rotor spinning on its axis.

Torque is calculated as the product of vectors of tangential force and the radius from the axis to the air gap, and instantaneous torque is the torque at a moment integrated with respect to a mechanical angle of 360°. The tangential force varies with the position of the stator and rotor, and this force causes instantaneous torque and the sources of torque change. Therefore, it is important to spatially analyze B_r, B_t, and F_t.

The magnetic flux density and tangential force, the sources of torque, were compared and analyzed, and the impact of slot harmonics on torque was investigated in this study. This study is divided into four stages for all slot combinations, as shown in Fig. 3, and each stage is represented by a box of dashed lines. (1) The magnetic flux density obtained through finite element analysis was decomposed into radial and tangential components, and a fast Fourier transform (FFT) was conducted for both components. (2) The harmonic orders of the tangential force were obtained by using the Maxwell stress tensor

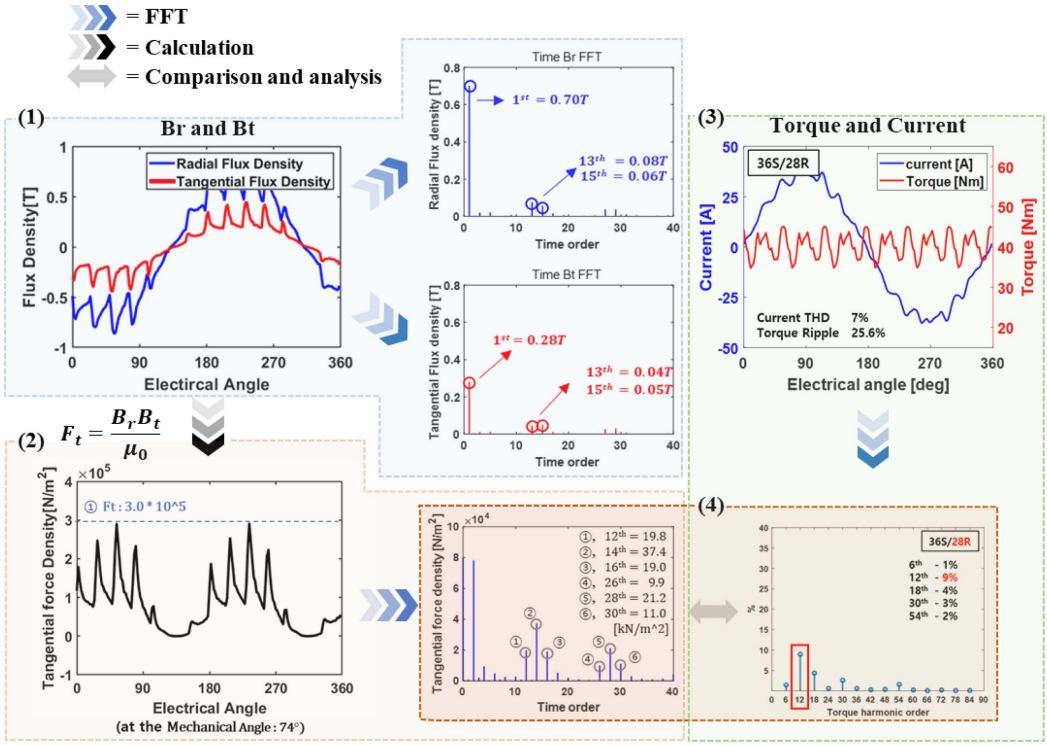

Fig. 3. (Color online) Analysis flowchart of torque characteristics with the following four steps, (1) B_r and B_t in time and their FFT, (2) calculation of F_t and its FFT, (3) torque in time and its FFT, (4) comparison of F_t and torque regarding their FFT.

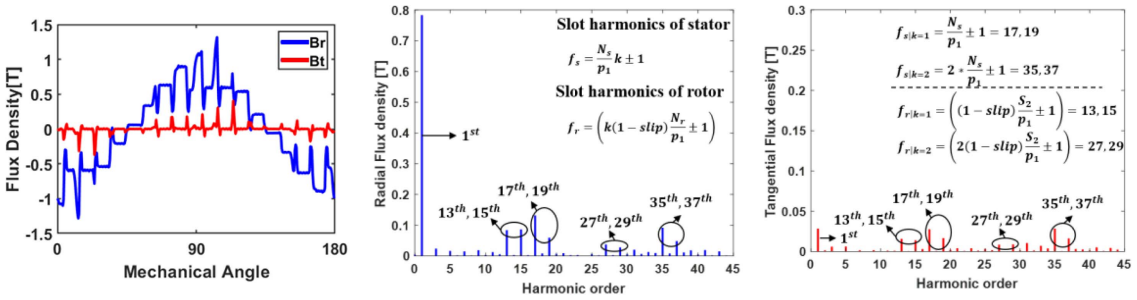

Fig. 4. (Color online) Spatial magnetic flux density in the air gap: (a) magnetic flux density in radial and tangential directions; (b) slot harmonic orders of B_r; (c) slot harmonic orders of B_t.

method. (3) The orders of the instantaneous torque were acquired in the previous stage. (4) A. Harmonic components that dominate the torque ripple among the harmonics of F_t were identified by comparing the harmonics of F_t and torque ripple, and the favorable number of slots in a motor needed to suppress torque ripple was selected. B. Harmonic components that dominate the torque ripple among the harmonics of F_t were determined by comparing the harmonics of F_t and torque ripple, and the number of slots in a motor reducing torque ripple was selected.

4.1. Spatial Analysis of Magnetic Flux Density in the Air Gap

The magnetic flux density divided into two vectors in the tangential and radial directions is distributed in space (θ) and time (t). In this section, the spatial variation of the magnetic flux density is analyzed at a given time, and its temporal distribution is discussed in the following section. Because a four-pole motor has two electrical cycles for one spin of a rotor, the waveforms of B_r and B_t are given for 180 mechanical degrees, as shown in Fig. 4(a). Note that B_r is much larger than B_t because flux passes across an air gap between the pole surfaces of the stator and rotor. However, the torque proportional to the tangential force is determined by the product of B_r and B_r; hence, the rates of change of both flux densities with respect to rotor slot number should be considered in terms of their impact on torque ripple.

In Figs. 4(b) and 4(c), the FFT of B_r and B_r with respect to space proves the existence of slot harmonics coming from the stator and rotor, as calculated in Table 1. A slot number of 36 in the stator leads to the 17th and 19th harmonics ($k = 1$) and higher orders ($k \geq 2$). Similar to the stator, the 13th, 15th, and higher harmonics are generated by the 28 rotor slots at the same time.

The magnetic flux density of the 11 models in Fig. 2 was analyzed in the same way as the base model with a 36-slot stator and a 28-slot rotor combination. Fig. 5 shows the FFTs of B_r and B_r and their spatial slot harmonics with respect to two factors, a harmonic order and a slot number, grouped by a dashed line in terms of the integer k. In addition, the division of harmonics by

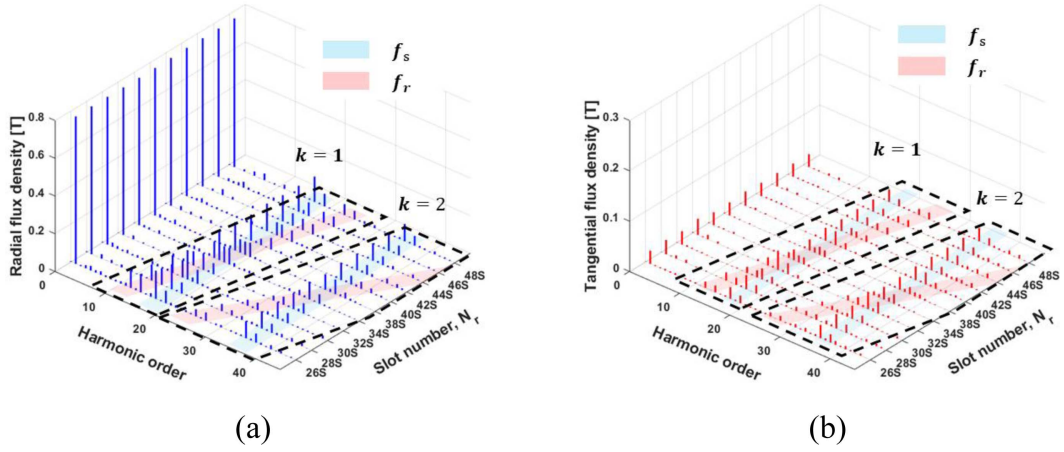

Fig. 5. (Color online) Spatial slot harmonic orders of the magnetic flux density for 11 models: (a) slot harmonic orders of B_r; (b) slot harmonic orders of B_t.

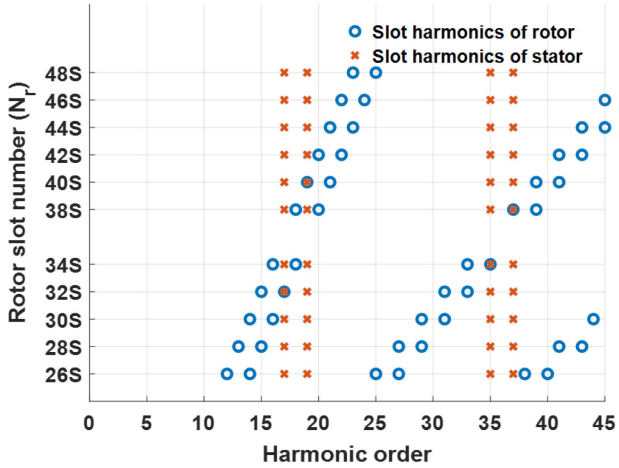

Fig. 6. (Color online) Calculation of slot harmonics of B_r and B_t in the motor for 36-stator-slot models.

either f_s (stator slot harmonics) or f_r (rotor slot harmonics) is useful for investigating the origin of each harmonic component, and the groups of f_s and f_r are shaded in blue and red, respectively. Considering the four blue-shaded regions in Figs. 5(a) and 5(b), one can see that no change in the slot number in the stator leads to the same arrangement of harmonic orders. However, there is an increase in f_r in terms of its harmonic order as the slot number increases from 26 to 48. In particular, the slope of $k = 2$ is double that of $k = 1$ in f_r. Fig. 6 shows the slot harmonic orders coming from the stator and rotor as calculated by equations (1) and (2); in the case of slot numbers of 32, 34, 38, and 40, their stator and rotor have one of the orders in common among the 17th, 19th, 35th, and 37th slot harmonics. In Table 3, the 17th and 19th components of B_r and B_r in each slot number are provided

Table 3. Magnitudes of 17th and 19th orders in B_r and B_t for 36-stator-slot models.

N_r	Radial flux density [T]		Tangential flux density [T]	
	17th	19th	17th	19th
26	0.150	0.066	0.023	0.015
28	0.132	0.059	0.028	0.017
30	0.155	0.075	0.022	0.014
32	0.086 (62 %)	0.058	0.038 (152 %)	0.022
34	0.159	0.087	0.021	0.014
38	0.150	0.070	0.022	0.016
40	0.138	0.033 (50 %)	0.025	0.027 (159 %)
42	0.146	0.070	0.024	0.015
44	0.139	0.065	0.024	0.017
46	0.137	0.072	0.024	0.014
48	0.134	0.066	0.024	0.014
Average	0.139	0.066	0.025	0.017

to scrutinize the slot numbers of 32 and 40 having one of the two harmonics in common, and the average is given at the bottom of the table. The 17th harmonics of B_r and B_t in the 32-slot rotor are 62 % and 152 %, respectively, compared to the average of 0.139 and 0.025 T, respectively. In the case of the 40-slot rotor, B_r and B_r have magnitudes of 50 % and 159 % in their 19th harmonics compared to the average of 0.066 and 0.017 T, respectively. Because of the coincidence of a specific harmonic order, it can be concluded that approximately half the reduction of B_r can be attributed to its corresponding order, and B_r has a magnitude that is a factor of ~1.5 higher than that of the average in a given harmonic.

4.2. Analysis of the Tangential Force Density

4.2.1. Slot Harmonics of the Stator and Rotor for Tangential Force Density

Because the tangential force density (F_t) is calculated based on equation (6), F_t is affected by the magnetic flux density in both the radial and tangential directions. Figs. 5(a) and 5(b) show the slot harmonics of B_r and B_r. The F_t harmonics generated by the combination of B_r and B_r can be divided into two terms by calculating n and m given in two magnetic flux densities:

$$F_t(t_M,\ \theta) = \frac{B_r(t_M,\ \theta)B_t(t_M,\ \theta)}{\mu_0}$$

$$= \frac{1}{\mu_0}[\Sigma_{n=1}^{\infty}B_{r(n)}\cos(\omega t_M - n\theta)\Sigma_{m=1}^{\infty}B_{t(m)}\cos(\omega t_M - m\theta)]$$

$$= \frac{1}{2\mu_0}[\Sigma_{n=1}^{\infty}\Sigma_{m=1}^{\infty}B_{r(n)}B_{t(m)}$$

$$[\cos((m-n)\theta) + \cos(2\omega t_M - (m+n)\theta)]]\,. \quad (7)$$

The magnitude of an F_t harmonic is determined by the product of the nth order in B_r and the m_{th} order in B_r. In Fig. 5(a), the magnitude of a fundamental wave is estimated to be ~50 % of B_r, and the average of a fundamental wave in B_r is a factor of 26.4 higher than that in B_r. Therefore, any harmonic wave in B_r combined with a fundamental wave in B_r become a dominant harmonic wave in F_t. Even though the 17th and 19th stator slot harmonic waves ($k = 1$) exist in B_r and B_t, as shown in Fig. 5, B_r is the magnetic flux density becoming an F_t harmonic wave by combining with a fundamental wave in B_r. In Fig. 7, this calculation process is detailed from the perspective of harmonic order, and the 17th and 19th slot harmonic waves turn into the 16th, 18th, and 20th harmonic waves in F_t by a fundamental wave in B_r. Because the 18th order positioned in the middle of three orders is affected by both the 17th and 19th orders, it has a greater influence

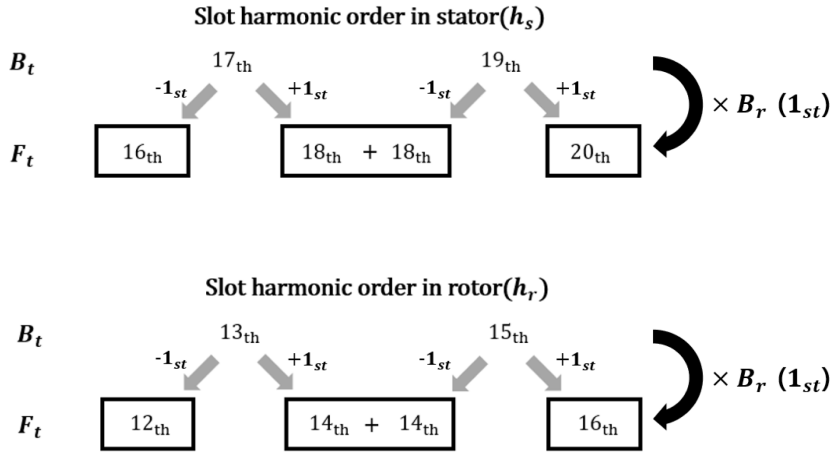

Fig. 7. Calculation process of harmonic orders from B_r and B_t to F_t.

on torque than the 16th and 20th orders.

The 16th, 18th, and 20th orders are represented as the F_t slot harmonic wave (k = 1), and the F_t slot harmonic wave can be expressed by

$$h_s^{Ft(-)} = k\frac{N_r}{p} - 2\,,\; h_s^{Ft(0)} = k\frac{N_r}{p}\,,\; h_s^{Ft(+)} = k\frac{N_r}{p} + 2 \qquad (8)$$

based on equation (1). A rotor slot harmonic wave also has three harmonic orders with respect to k:

$$h_r^{Ft(-)} = k(1-slip)\frac{N_r}{p} - 2\,,\; h_r^{Ft(0)} = k(1-slip)\frac{N_r}{p}\,,$$

$$h_r^{Ft(+)} = k(1-slip)\frac{N_r}{p} + 2\,, \qquad (9)$$

which are calculated from equation (2).

To understand the characteristics of an F_t harmonic wave with respect to slot combinations, slot harmonic waves obtained by equations (8) and (9) are shown in Fig. 8. Because the two harmonic waves of B_r and B_t for all slot combinations become the three harmonic waves of F_t, the number of orders in common for the stator and rotor in F_t are increased compared to those in B_r and B_t. In the case of the 32 and 40 rotor slots (k = 1) having two orders in common, as shown in Fig. 6, they have four orders (16th, 18th orders and 18th, 20th orders), as shown in Fig. 8. There is one order of F_t harmonics in common for the 28 and 44 rotor slots, even though these models do not have any orders in common for the harmonics of B_r and B_t. Thoroughly observing the FFT of tangential force density is important for investigating the effect on torque when the stator and rotor have harmonic orders in common.

4.2.2. Analysis of Tangential Force Density

The tangential force density (F_t) is calculated using the

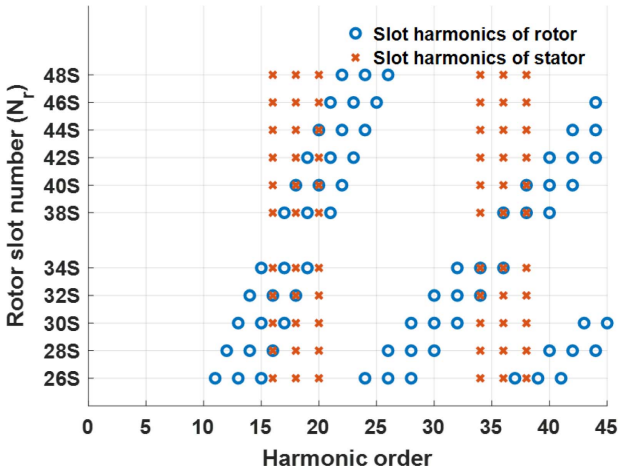

Fig. 8. (Color online) Calculation result for F_t slot harmonics with respect to slot combinations of 26 to 48.

magnetic flux density of the air gap in two different directions, and F_t was investigated through the FFT. In Fig. 9(a), $B_r(t_0, \theta)$, $B_t(t_0, \theta)$, and $F_t(t_0, \theta)$ generated in the air gap with a mechanical angle of 180° at the maximum torque are plotted at the same time, and Fig. 9(b) shows only the F_t distribution. Note that F_t calculated with B_r and B_t is greatly influenced by the magnitude of B_r and the rate at which B_t changes, as shown in Fig. 9(a). The FFT of the tangential force densities for the 11 models including the base model is performed to study the characteristics of F_t.

Figure 10 shows all the components of the F_t harmonic wave including harmonic orders given in Fig. 8 with respect to slot combinations. There are larger F_t values in case of having orders in common than in the others. The magnitudes of the harmonic waves are listed in Table 4 based on 16th, 18th, and 20th orders to observe the change of magnitude in harmonics with respect to slot

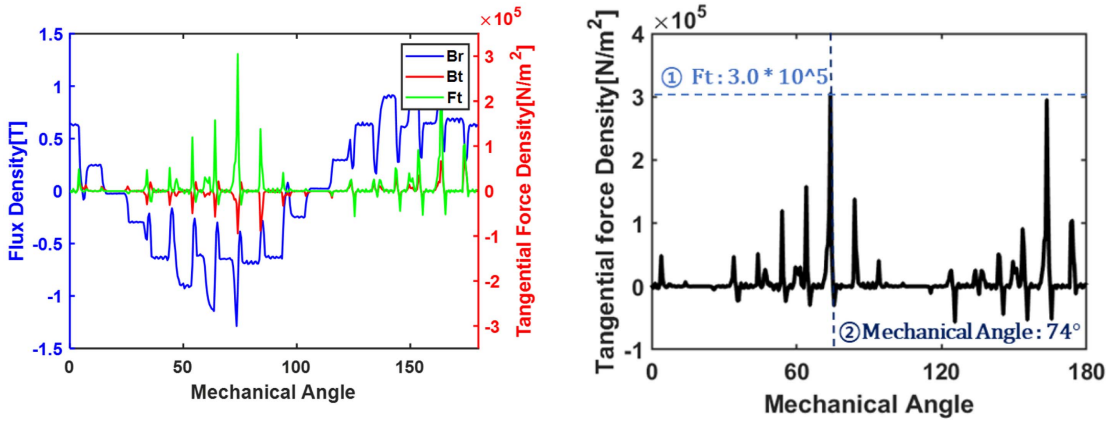

Fig. 9. (Color online) Radial (B_r) and tangential (B_t) magnetic flux density and tangential force density (F_t) in space: (a) B_r, B_t, and F_t; (b) F_t.

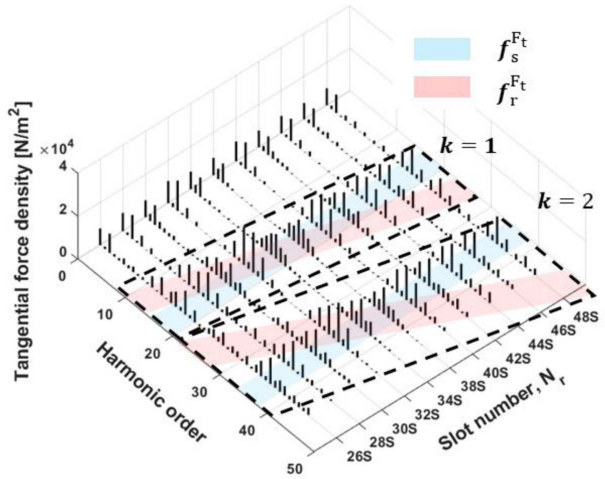

Fig. 10. (Color online) Slot harmonic orders of a tangential force density for 36-stator-slot models.

combinations. The average value of harmonic waves in the 16th, 18th, and 20th orders are 8988, 12734, and 7214 N/mm^2, respectively, and the magnitudes of harmonics in the 32- and 40-slot rotors having two orders in common are from 122 % to 197 % higher than average values. Even though F_t is instantaneous tangential force density, having a large value related directly to the magnitude of torque implies a large torque ripple because of the value at the moment generating the maximum torque. Therefore, the 32- and 40-slot rotors have a larger torque ripple than the others, as presented in Table 4.

4.3. Torque Characteristics

Torque is defined through a calculation with not only the tangential force density but also the back EMF and current. The torque can be calculated using the back EMF distributed spatially (θ) and time-varying current:

Table 4. Magnitudes of 16th, 18th, and 20th orders in F_t harmonics for 36-stator-slot models.

N_r	Tangential force density N/mm^2		
	16th	18th	20th
26	7108	11078	5503
28	9888	13177	7000
30	7787	10810	5269
32	17695 (197 %)	18700 (147 %)	10522 (146 %)
34	7071	11392	5381
38	6619	11610	6382
40	10927 (122 %)	16986 (133 %)	13595 (188 %)
42	7627	11301	4935
44	9077	11972	9840
46	7848	11081	4998
48	7226	11966	5929
Average	8988	12734	7214

$$T_e = \frac{3}{2\omega_m}[E_m I_m \cos\theta - E_{m5} I_m \cos(6\omega t - \theta_5) + E_{m7} I_m \cos(6\omega t - \theta_7)\cdots]. \quad (10)$$

Note that the orders of multiples of six in torque are major factors in a three-phase induction motor [12]. The relation between the harmonic components of B_r, B_t, and F_t and torque and torque ripple can be investigated by comparing with the harmonics of multiples of six in torque and F_t harmonic orders.

4.3.1. Analysis of Torque Ripple

The torque and current waves for the 11 models are plotted in Fig. 11. Current waveforms with respect to slot combinations are shown on the right side of the figure. Because some of the models have harmonic waves in the current waveforms, these harmonics are reflected in the

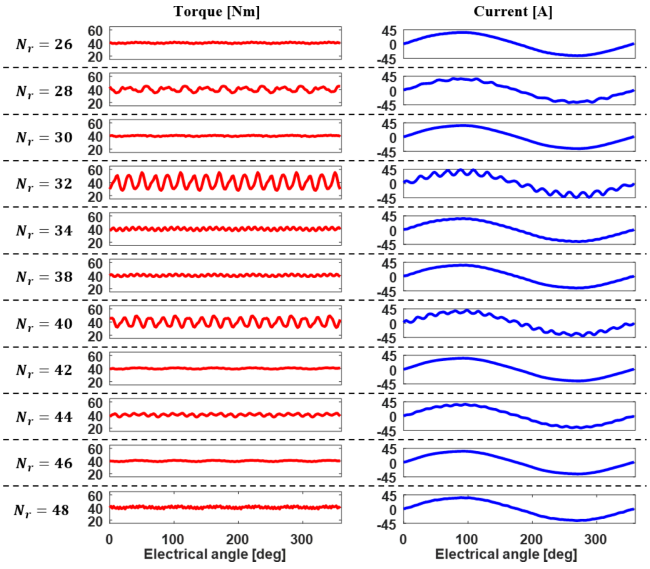

Fig. 11. (Color online) Torque and current waveforms for 36-stator-slot models.

torque waveforms. The 32- and 40-slot rotors with heavily distorted currents have the worst torque ripple, and there are also significant torque ripple and distorted current waveforms for the 28- and 44-slot rotors. The torque ripple shown in the figure is influenced by the instantaneous torque, which is the integrated torque generated at a specific point of the air gap for one period in the mechanical angle [11].

$$\left|\vec{T}(\alpha)\right| = \int_0^{360^\circ} \left|\vec{F}_t\right| \cdot A \cdot r \, d\theta. \tag{11}$$

where A and r are the area of air gap and a radius from the center of a shaft to the middle of air gap, respectively. Because the torque ripple is directly related to F_t, the harmonics of torque and F_t are compared and analyzed.

The harmonic orders and magnitude of harmonics in the torque are plotted in Fig. 12. The harmonic orders of torque have multiples of six except for a fundamental wave, as given in equation (10), and the sixth orders in all combinations have almost the same magnitude. The 18th orders in the 32- and 40-slot rotors have the highest value, and there are all different harmonic orders generated with respect to slot combinations. For this reason, it is necessary to compare the torque ripple and harmonic orders in all combinations, even though the magnitude of the harmonics is important. Table 5 lists the harmonics in torque and the rotor harmonic orders in F_t. Toque ripples with respect to slot combinations are on the left side of the table, and the harmonic orders of torque and the maximum value among those are shown in orange. Also listed are the rotor harmonic orders of F_t in the case of k from 1 to 4, and common orders in the stator and rotor among F_t harmonics described in Fig. 10 are presented in red. Hereafter, the

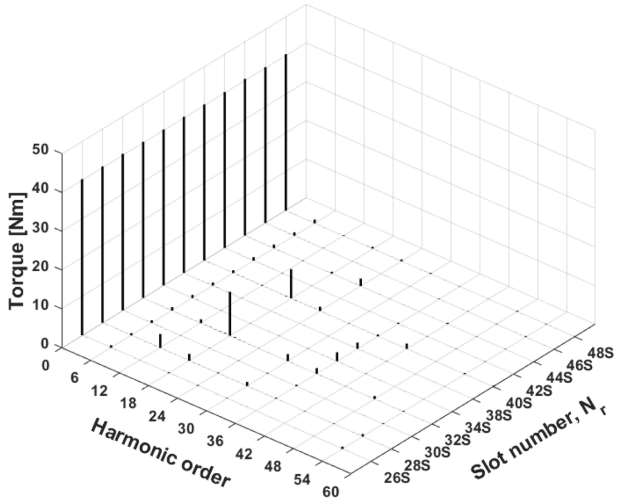

Fig. 12. F_t harmonic orders and the magnitude of harmonics for 36-stator-slot models.

Table 5. (Color online) Characteristics of torque and the F_t harmonic order of a rotor for 36-stator-slot models.

N_r	Torque ripple [%]	Torque harmonic		F_t harmonic order			
		Order	Major order	$k=1$	$k=2$	$k=3$	$k=4$
26	7.5	6, 54	54	11, 13, 15	24, 26, 28	37, 39, 41	50, 52, 54
28	25.6	6, 12, 18	12	12, 14, 16	26, 28, 30	40, 42, 44	54, 56, 58
30	5.9	6	6	13, 15, 17	28, 30, 32	43, 45, 47	58, 60, 62
32	68.4	6, 12, 18	18	14, 16, 18	30, 32, 34	46, 48, 50	66, 68, 70
34	14.6	6, 36	36	15, 17, 19	32, 34, 36	49, 51, 53	70, 72, 74
38	10.9	6, 36	36	17, 19, 21	36, 38, 40	54, 56, 58	74, 76, 78
40	44.6	6, 18, 24	18	18, 20, 22	38, 40, 42	58, 60, 62	78, 80 ,82
42	5.5	6	6	19, 21, 23	40, 42, 44	61, 63, 65	82, 84, 86
44	14.2	6, 24	24	20, 22, 24	42, 44, 46	64, 66, 68	86, 88, 90
46	5.6	6	6	21, 23, 25	44, 46, 48	67, 69, 71	90, 92, 94
48	12.8	6, 18, 24, 72	72	22, 24, 26	46, 48, 50	70, 72, 74	94, 96, 98

Table 6. (Color online) Combination of 24 stator slots for the comparative study.

Number of poles	Number of slots in stator	Number of slots in rotor
4	24	16, 18, 20, 22, 26, 28, 30, 32, 34, 36

Table 7. Characteristics of torque and the F_t harmonic order of a rotor for 24-stator-slot models.

N_r	Torque ripple [%]	Torque harmonic		F_t harmonic order			
		Order	Major order	$k=1$	$k=2$	$k=3$	$k=4$
16	45.0	6, 12, 18	6, 12	6, 8, 10	14, 16, 18	22, 24, 26	30, 32, 34
18	9.7	6, 12, 36	36	7, 9, 11	16, 18, 20	25, 27, 29	34, 36, 38
20	92.0	6, 12, 18	12	8, 10, 12	18, 20, 22	28, 30, 32	38, 40, 42
22	9.7	6, 24	24	9, 11, 13	20, 22, 24	31, 33, 35	42, 44, 46
26	6.8	6, 24	24	11, 13, 15	24, 26, 28	37, 39, 41	50, 52, 54
28	70.8	12, 18, 30	12	12, 14, 16	26, 28, 30	40, 42, 44	54, 56, 58
30	7.5	6, 30, 60	60	13, 15, 17	28, 30, 32	43, 45, 47	58, 60, 62
32	19.6	6, 12, 18	18	14, 16, 18	30, 32, 34	46, 48, 50	62, 64, 66
34	16.3	6, 36	36	15, 17, 19	32, 34, 36	49, 51, 53	66, 68, 70
36	32.0	6, 12, 36	36	16, 18, 20	34, 36, 38	52, 54, 56	70, 72, 74

orders in the common generation in the stator and rotor are referred to as "a common order" or "common orders." The reason for the different torque ripples generated from 5.5 % to 68.4 % is explained by using the harmonic orders of torque, B_r, B_t, and F_t. Because the stator and rotor have two common orders in F_t harmonics (k = 1), the 32- and 40-slot rotors have the worst torque ripples. The two models have 16th and 18th orders and 18th and 20th orders as common orders, respectively, and the 18th order occurs in both models. This 18th order in the F_t harmonic is dominant on the torque ripple, as shown in the table in orange. The 18th order is calculated by using the fundamental, 17th, and 19th harmonics in the magnetic flux density, as described in equation (7). The 32-rotor-slot model has worse torque ripple than the 40-rotor-slot model, even though they have the largest torque ripple under the same conditions, because the 32-rotor-slot model has a lower common order than the 40-rotor-slot model. For the 28- and 44-rotor-slot models having one common order in F_t harmonics (k = 1), these models give different results from those of the 32- and 40-rotor-slot models. The 28-rotor-slot model has a large torque ripple (25.6 %) because of having a 16th order in common, but a dominant order is not a 16th order but a 12th order (see the orange shaded column). The 44-rotor-slot model has a smaller torque ripple (14.2 %) than the 28-rotor-slot model because its 24th order for the rotor slots is higher than that of the 12th order for the 28 rotor slots. There are two models with two common orders in the case of k = 2 (34 and 38 rotor slots), and the 36th harmonic order is one of the common orders for those models. Because the 34- and 38-rotor-slot models have two common orders (k = 2) and a magnitude difference, these models have 14.6 % and 10.9 % torque ripples, respectively, despite having the same conditions as the 32- and 40-rotor-slot models. The 48-rotor-slot model has three common orders in the case of k = 3, and the 72nd order is the dominant one among them. However, this model has a 12.8 % torque ripple because of its high harmonic order. The 26-rotor-slot model has a 54th order in common in the case of k = 4, and this order is dominant in the torque. The 30-, 42-, and 46-rotor-slot models exhibit greatly reduced torque ripple because they have only a sixth harmonic order as the dominant one.

The correlation between torque ripple and the component of harmonics in torque and F_t is described using 11 rotor models with 36 stator slots fixed. Additional analysis for 24-stator-slot models will be performed in the following section to generalize the results of the 36-stator-slot models.

4.3.2. Analysis of 24-Slot-Stator Model

A 24-stator-slot model having the same magnetic flux density in teeth with 36 stator slots was designed to prove the correlation between torque ripple and the component of harmonics in torque and F_t for the 24 stator slots. A 24-stator-slot model with the same total winding turns, cross-sectional area, and lamination length as that with 36 stator slots was created. The slot combinations of a rotor were selected through the same process as for the 36-stator-slot model, as given in Table 6.

Ten models with 24 fixed stator slots were analyzed in the same way as for the 36-stator-slot model, and the harmonic orders of torque and F_t in a rotor are listed in

Table 7. The maximum orders among the torque harmonics are given with orange shading, and the common orders of F_t harmonics are listed in red. Because two common orders in F_t harmonics (k = 1) occur, the 20-and 28-rotor-slot models have the worst torque ripple. The two models have a larger torque ripple than the others, but the reason why the 20-rotor-slot model has a larger torque ripple than the 28-rotor-slot model is because the former has a lower common order than the latter. The 16- and 32-rotor-slot models exhibit a larger torque ripple because they have one common order in F_t harmonics (k = 1). In addition, the torque ripple for 16 rotor slots is greater than that for 32 rotor slots because the 16-rotor-slot model has a lower dominant order in torque than the latter. The 36-rotor-slot model has a large torque ripple (32 %) and common orders with the 34th, 36th, and 38th harmonics at k = 2 and 70th, 72nd, and 74th harmonics at k = 4. The worst torque ripple occurs in the case of two common orders in F_t harmonics (k = 1) and a larger torque ripple in the case of a common order in F_t harmonics (k = 1) than slot combinations in both 36- and 24-stator slot models.

5. Conclusion

In this study, the correlations between torque ripple and harmonic orders of varying magnetic flux density obtained by slot combinations are described. The 36 and 24 stator slots exhibited the worst torque ripple in the case of two common orders in F_t harmonics (k = 1), and considerable torque ripple occurred in the case of a common order in F_t harmonics (k = 1). The harmonic orders of the stator and rotor were calculated using equations (8) and (9), and slot combinations having the worst or considerable torque ripple were identified using these two equations. The worst torque ripple occurred when there was more than one common order in F_t harmonics (k = 1) and there was deteriorated torque when there was more than one common order in F_t harmonics ($k \geq 2$). Therefore, avoiding slot combinations with the worst torque ripple and selecting slot combinations that are appropriate for applications are important.

Acknowledgments

This research was supported by Korea Electric Power Corporation (Grant number: R19XO01-12) and Basic Science Research Program through the National Research Foundation of Korea funded by the Ministry of Education (Grant number : NRF- 2018R1D1A1B07049717).

References

[1] G. Joksimović, M. Mezzarobba, A. Tessarolo, and E. Levi, IEEE Access **8**, 135558 (2020).
[2] T. Gundogdu, Z. Q. Zhu, J. C. Mipo, and P. Farah, ICEM, 419 (2016).
[3] T. Gundogdu, Z. Q. Zhu, J. C. Mipo, and P. Farah, ICEM, 391 (2016).
[4] M. Mach, R. Cipin, M. Toman, and V. Hajek, EEEIC/I&CPS Europe, 1 (2018).
[5] M. Valtonen, A. Parviainen, and J. Pyrhonen, IEEE International Electric Machines & Drives Conference **1**, 668 (2007).
[6] J. Le Besnerais, V. Lanfranchi, M. Hecquet, and P. Brochet, IEEE Trans. Mag. **45**, 3131 (2009).
[7] T. Kobayashi, F. Tajima, M. Ito, and S. Shibukawa, IEEE Trans. Mag. **33**, 2101 (1997).
[8] G. Joksimović, E. Levi, A. Kajević, M. Mezzarobba, and A. Tessarolo, IEEE Access **8**, 228572 (2020).
[9] G. Y. Zhou and J. X. Shen, IEEE Trans. Ind. Appl. **53**, 134 (2016).
[10] I. Boldea and S. Nasar, The Induction Machines Design Handbook, Electric Power Engineering Series. Taylor & Francis (2009).
[11] J. F. Gieras, Permanent magnet motor technology: design and applications. CRC press (2018).
[12] A. Najmabadi, W. Xu, and M. Degner, IEEE IEMDC 1 (2017).